International Journal of Heat and Fluid Flow 31 (2010) 201–207

Contents lists available at ScienceDirect

International Journal of Heat and Fluid Flow

journal homepage: www.elsevier.com/locate/ijhff

Flow boiling enhancement on a horizontal heater using carbon nanotube coatings

N. Singh, V. Sathyamurthy, W. Peterson, J. Arendt, D. Banerjee *

Department of Mechanical Engineering, Texas A&M University, College Station, TX 77843, United States

ARTICLE INFO

Article history:
Received 2 August 2008
Received in revised form 7 September 2009
Accepted 7 November 2009
Available online 27 January 2010

Keywords:
Nanotechnology
Flow boiling
Heat transfer enhancement
Multi walled carbon nanotubes (MWCNT)
Chemical vapor deposition
Multi phase flows

ABSTRACT

In this study we measure the flow boiling heat flux on a horizontal heater that is heated from below. The horizontal heater consists of either a bare silicon wafer or a silicon wafer that is coated with multi walled carbon nanotubes (MWCNT). The silicon wafer is clamped on a constant heat flux type calorimeter consisting of a vertical copper cylinder with embedded cartridge heaters and K-type thermocouples. De-ionized (DI) water was used as the test fluid. The calorimeter apparatus is housed in a test section with glass walls for visual observation. The liquid is pumped from a constant temperature bath to maintain a fixed subcooling during the experiments under steady state conditions.

Boiling curves (wall heat flux as a function of heater temperature) were obtained for different flow rates and liquid subcooling. Experiments were performed for two different flow rates and two different liquid subcoolings. Flow boiling heat flux was enhanced by as much as 180% at boiling incipience for silicon substrates coated with carbon nanotubes. MWCNT was less effective in enhancing heat flux as the flow rate and liquid subcooling was increased. This anomalous behavior was explained using flow boiling models reported in the literature.

1. Introduction

Boiling is a highly non-linear phenomenon with strong coupling of the governing transport mechanisms (thermal and hydro-dynamic interactions). Apart from the fluid and heater thermo-physical properties, the variables affecting boiling heat flux include wall superheat, spatial distribution of nucleation site density (Zhang and Shoji, 2003), spatial distribution of bubble departure diameter, contact angle, heater orientation, gravity, etc. (Dhir, 1993, 1998). Flow boiling is affected by additional operational parameters such as flow velocity, flow boiling regimes, quality (and void fraction), surface features, operating pressure, pressure drop in liquid phase and vapor phase (Carey, 2007).

Flow boiling enhancement has been explored in the literature using micro-scale as well as macro-scale features in round tubes, e.g., cruciform tube, internally finned tube and helically grooved tube. Non-circular features have also been reported in the literature such as plate fin surface, micro-fins, twisted-tape inserts, offset or perforated fins and cross-ribbed surface (Carey, 2007; Webb, 1994; Thome, 1990). In addition, reducing the hydraulic diameter (D_h) can enhance the heat transfer coefficient (h) in single phase and two phase flow configurations (e.g., $h \times D_h^{-1}$ in single phase laminar flow for both constant temperature and constant heat flux boundary conditions), but this is also at the expense of an even higher pressure penalty (e.g., $\Delta p \times D_h^{-4}$ at constant volume flow rate in single phase laminar flow).

Recently, nano-structured surfaces were shown to enhance pool boiling heat flux. Pool boiling heat fluxes were enhanced by 30–300% on heaters coated with multi walled carbon nanotubes (MWCNT) using dielectric coolants (Ahn et al., 2006a,b). Silicon wafers were coated with MWCNT using chemical vapor deposition (CVD) process (Zhang et al., 2004). The augmentation of pool boiling heat flux was observed to depend on the wall superheat, subcooling and the height of the MWCNT. MWCNT of two different heights were used: 9 and 25 μm. Both types of MWCNT enhanced nucleate boiling heat transfer by 30–60%. In contrast, the MWCNT of 25 μm height enhanced film boiling heat transfer by 60–300% while the 9 μm MWCNT did not cause any significant enhancement. Prior numerical and experimental investigations (e.g., Banerjee and Dhir, 2001) predicted that for film boiling of refrigerant PF-5060 the minimum vapor film thickness is ~15 μm. Hence the 25 μm MWCNT possibly disrupted the vapor film and enhanced the heat transfer while the 9 μm MWCNT did not.

The different mechanisms responsible for enhancement of flow boiling heat transfer on nano-structured surfaces and their relative contribution to the total heat transfer are the subject of this study. The length scales affecting the physical mechanisms in boiling range from nm to cm. The conventional mechanistic models for boiling are based on continuum regime (Carey, 2007) and are not applicable to non-continuum regimes that occur during boiling on nano-structured surfaces. For example Hsu's criteria for bubble nucleation theory (Carey, 2007) cannot be applied to

* Corresponding author. Tel.: +1 979 845 4500; fax: +1 979 845 3081.
E-mail address: dbanerjee@tamu.edu (D. Banerjee).

0142-727X/$ - see front matter © 2009 Elsevier Inc. All rights reserved.
doi:10.1016/j.ijheatfluidflow.2009.11.002

Nomenclature

C_{sf}	surface constant for boiling correlation	Re	reynolds number (for liquid flow only)
D_h	hydraulic diameter = 4 times area of flow cross section/ wetted perimeter of flow	T_1	temperature at thermocouple location 1
		T_2	temperature at thermocouple location 2
h_{lv}	enthalpy of phase change (from liquid to vapor)	T_w	wall temperature (or temperature on the boiling surface)
k	thermal conductivity		
l	liquid property	Δx	distance between thermocouple location
ONB	onset of nucleate boiling, property value at ONB	ω	measurement uncertainty of an experimental parameter
p	pressure		

nano-structured surfaces. Hence additional experimental data are needed to support new theories that are required for predicting the boiling phenomena on nano-structured surfaces.

Kim et al. (2001) measured the thermal conductivity of MWCNT to be in excess of 3000 W/mK. Therefore, the potential mechanisms for heat transfer enhancement can be categorized to be primarily due to scale effects (e.g., high surface area per unit projected area or the "nano-fin" effect) and due to material property effects. These effects can be itemized as follows (Ahn et al., 2006a,b).

The MWCNT structures serve as enhanced heat transfer surfaces ("nano-fins") which can augment the effective area of the heater surface and enhance conduction and convection.

The higher thermal conductivity of Carbon Nano-Tubes (6) can also enhance transient conduction to the liquid phase from the heater surface (during periodic liquid–solid contacts after each vapor bubble departure event).

In the nucleate boiling regime – the MWCNT structures disrupt the "thermal micro-layer" region under the bubbles enhancing mixing and thermal transport. The MWCNT structures disrupt the vapor layer in film boiling causing periodic quenching of the heater.

Additionally "cold spots" (Banerjee and Dhir, 2001) that form on a boiling surface (due to coupled non-linear thermal and hydro-dynamic interactions) can be enhanced by MWCNT. This leads to spatio-temporal re-distribution of the wall temperature which can enhance the boiling heat flux.

In subsequent studies Sririaman and Banerjee (2007) employed silicon substrates with nano-fins chemically etched out of the silicon substrate using Step and Flash Nano-Imprint Lithography (SFNIL) process. The height of the silicon nanofin arrays were varied parametrically for each substrate (keeping the pitch and diameter constant) to verify the effect of the material properties of the surface nano-structures on pool boiling heat flux. The thermal conductivity of silicon is 150–200 times smaller than MWCNT. Therefore, if the conductivity effects dominate the enhancement of pool boiling heat flux – silicon nanofins should demonstrate a lower enhancement than compared to surfaces coated with MWCNT. However, from experimental measurements it was observed that silicon nanofins enhanced the critical heat flux (CHF) by 120% and the enhancement was independent of the height of nano-fins for nano-fin heights exceeding 100 nm. In contrast MWCNT enhanced CHF by only 60%. The silicon nanofins were of 200 nm in diameter with a pitch of 900–1000 nm and had fixed heights ranging from 100 nm to 600 nm for each substrate used in the study. In contrast, MWCNT had a random pitch of 16–40 nm with diameters of 8–16 nm and fixed heights of 9 μm or 25 μm. These results show that the enhancement of pool boiling heat flux is dominated by scale effects ("nano-fin" effect) rather than by material property effects. These results also allude to the fact that the thickness of the micro-layer thickness in nucleate boiling is ~100 nm or less.

In this work we report the enhancement of flow boiling heat flux on a horizontal heater using surface nano-structures. The surface nano-structures were obtained by in situ synthesis of carbon nanotubes on diced silicon wafers using chemical vapor deposition (CVD) techniques. This study is relevant for various thermal management applications in electronics chip cooling, energy conversion devices, cryogenic systems, energy storage, materials processing and futuristic applications (e.g., micro-channel cooling). An enhanced understanding of micro-scale and nano-scale features in flow boiling will enable the development of novel devices for thermal management.

2. Experimental setup

This study was designed for flow boiling in a macro-scale channel since micro-channel flow boiling is limited by the associated pressure penalty. Also, "edge effects" in small heaters can distort the boiling curve. Bakhru and Lienhard (1972) as well as Dhir and Lienhard (1973) showed that edge effects can dominate during boiling on "small" heaters. To eliminate distortions to the boiling curve from the edge effects the heater dimension should be larger than the boiling length scale, i.e., the "most dangerous" Taylor instability wave; as well as at least an order of magnitude larger than the capillary length (Carey, 2007). For properties of water the capillary length scale is ~2.5 mm and the boiling length scale is ~2.5 cm. This dictates that the size of the heater should be greater than 2.5 cm on each side. Hence, the heater size in this study was chosen to be 5 cm wide and 7.5 cm long. The height and width of the macro-channel was also chosen to be larger than the heater size to eliminate any distortions to the boiling curve from the "edge effects" arising from contributions from the side walls, top wall or bottom wall.

The experimental setup consists of the flow boiling test section, a constant temperature bath for pumping the working liquid and a data acquisition unit for recording the temperatures from the experimental apparatus. The constant temperature bath consists of a digital mode chiller-heater unit (Model 9602 circulator from PolySciences Inc.). The unit consists of a cubical storage tank with a stirrer (size 26 × 26 × 26 cm), a centrifugal pump which can be programmed for 5 different speeds ranging from 9 to 15 l/min, and a heat exchanger unit to digitally control the temperature of the bath. The bath temperature can be regulated from −25 °C to 150 °C. In addition two centrifugal pumps were used to pump DI water in and out from the constant temperature bath to the flow boiling test section. A flow meter (Model: FL1504A, Vendor: Omega) was used to measure the flow rate of liquid at the inlet of the test section.

The test section consists of a rectangular chamber housing the heater apparatus (calorimeter), along with the inlet and outlet for fluid flow. A schematic of the experimental setup is shown in Fig. 1. To eliminate wall effects that could potentially distort the flow boiling on the nano-structured surfaces, the test section configuration was realized utilizing a rectangular macro-channel of a square cross section of 10 cm × 10 cm and the length of the test section in the flow direction was 20 cm. A heater apparatus was

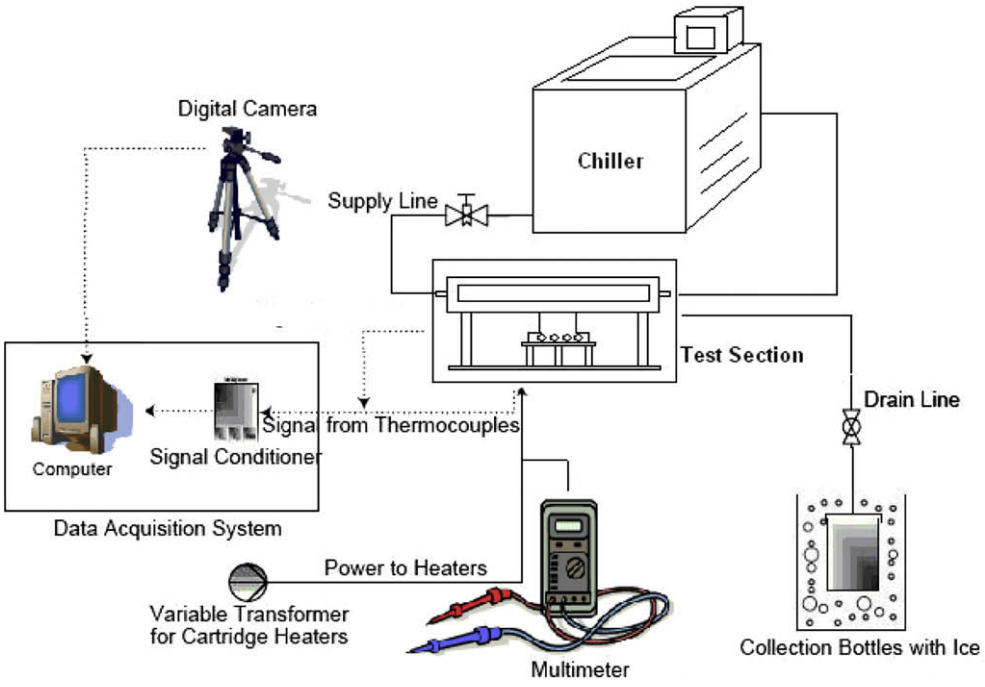

Fig. 1. Schematic diagram of the experimental setup.

placed at the bottom of the channel on which a silicon wafer (bare or coated with MWCNT) was mounted to serve as the flow boiling surface. This configuration was designed for future studies involving high speed digital image acquisition. Using atomically smooth silicon substrates in this study also helps to isolate the enhancement effects of MWCNT from variability introduced by random distribution of nucleating cavities on the side walls that can vary from surface to surface for commercially finished surfaces (e.g., copper). Flow boiling curves (wall heat flux as a function of heater temperature) are compared for bare silicon surfaces with that obtained for silicon surfaces coated with MWCNT.

The test section is made of aluminum and acetyl frames. Aluminum and acetyl were chosen for their rigidity, low coefficient of thermal expansion and for ease of machining of the frame. The top and the two sides of the test section were fitted with glass windows visual observation of the flow boiling regime as well as to perform high speed image acquisition of the bubble formation and departure process for future flow boiling studies. The copper block was heated using 750 W cartridge heaters. Total of eight cartridge heaters were embedded into blind holes that were horizontally machined in the vicinity of the bottom edge of the copper cylinder. The cartridge heaters are used to supply 6 kW of total heat input to the copper cylinder. The power to the cartridge heater was controlled using a DC power supply (ratings: 10 kW, 125 V, 53 A; Manufacturer: Amrel Inc.). Smaller blind holes were drilled horizontally and at various radial angles into the copper cylinder at 17 locations. K-type wire bead thermocouples were inserted in these holes to enable heat flux calculations in the vertical direction, as shown in Fig. 2. The K-type thermocouples are formed from wire bead junctions of Chromel and Alumel wires. K-type thermocouple was chosen for their superior linear response (the Seebeck coefficient varies by less than ±5%) in the temperature range of interest, chemical inertness at high temperatures (both chromel and alumel alloys are doped with silicon oxide for protection against oxidation) and broad range of operating temperature (from −300 °C to 700 °C). Five thermocouples inserted into the central plain of the calorimeter were used to estimate the heat flux values in the vertical direction. Two of the thermocouples are at the most narrow cross section (top section of the copper block) and are spaced 5 mm apart. The other three thermocouples are placed at a wider cross section (in the mid-section) which are separated by 5, 10.5 and 16 cm distances, as shown in Fig. 2.

The copper cylinder is mounted on a base plate below the test section. The base plate height is adjusted to keep the test surface (mounted on the copper cylinder) to be flush with the bottom surface of the test section. For example, during the experiments with the silicon wafer the height of the base plate is adjusted so that the silicon wafer surface is flush with the bottom surface of the test section.

Additional thermocouples are placed inside the test section to monitor the liquid temperature, the temperature of the ambient and the glass windows. All the thermocouples in the experimental apparatus are connected to a digital data acquisition system (NI-DAQ, Supplier: National Instruments). The NI-DAQ consists of an amplifier unit, a signal conditioning module, an isothermal terminal block and an M series multifunction device. The maximum sampling rate of the data acquisition apparatus is 100 kHz for 16 channels. Labview software (by National Instruments) was used to program and control the data acquisition unit from a desk top computer. To augment the capabilities for low noise and high bandwidth of the NI-DAQ unit, aluminum foils were used to cover the thermocouple wires and the foils were grounded to eliminate any noise captured from the ambient electro-magnetic interference (EMI) or surrounding electrical appliances in the laboratory.

3. Carbon nanotube (MWCNT) synthesis

Chemical vapor deposition (CVD) is a simple, cost-effective method of synthesizing nanotubes (single walled or multi-walled) on various substrates. Acetylene was used as the carbon pre-cursor gas with the sample being heated to 675–700 °C. A Lindberg/Blue M-tube furnace was employed for this purpose (the quartz tube in the furnace has a diameter of 7 cm). Iron layer of 10–20 nm thickness was vapor deposited on a silicon wafer (7.5 cm diameter) using an electron-beam mediated physical vapor deposition (PVD)

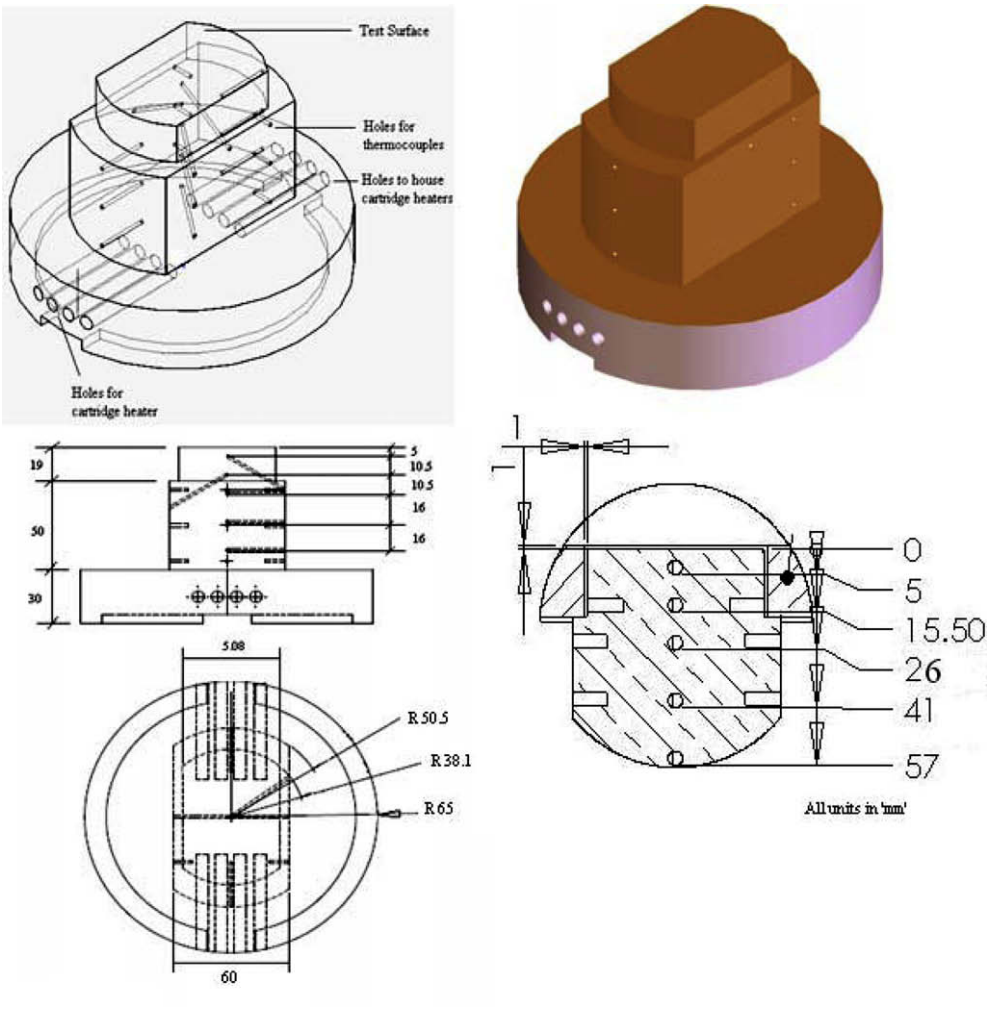

Fig. 2. Diagram showing the location of the inserted K-type thermocouples and the embedded cartridge heaters in the calorimeter apparatus consisting of the machined copper cylinder.

process. The iron acts as catalysis for the carbon nanotubes to nucleate and grow on the substrate. Prior to coating with MWCNT, the silicon wafer was then diced to a size of 5 cm × 7.5 cm. The diced substrate is placed in the mid-section of the quartz tube in the furnace. Gas flows through tubes to enter one end of the quartz tube in the furnace and flows along its axis and exits through an insulating glass wool plug placed at the opposite end. To prevent any contamination and to ensure safety the whole apparatus is placed in a negative pressure chamber (with respect to ambient) and negative gage pressure is maintained using an exhaust fan. Gas temperature in the furnace is measured using a K-type thermocouple. Nitrogen gas is used to purge the furnace of any oxygen at approximately 824 sccm for 20 min. Then the furnace is turned on, and heated to 200 °C. Then the temperature is raised by 50 °C increments in every 7 min to a final temperature of 700 °C. The furnace temperature is then allowed to stabilize and steady state is usually achieved in 30 min. Then acetylene flow is started into the quartz tube for one hour at 74 sccm. After acetylene exposure, nitrogen flow is reduced to 194 sccm to prevent oxidation during cool-down period. The height of the MWCNT coating is ~15–30 μm at the end of one hour of CVD synthesis. The diameters of the MWCNTs in the coating were found to vary randomly between 10 and 50 nm. Fig. 3 shows the top view of the MWCNT coating obtained by using a scanning electron microscope (SEM).

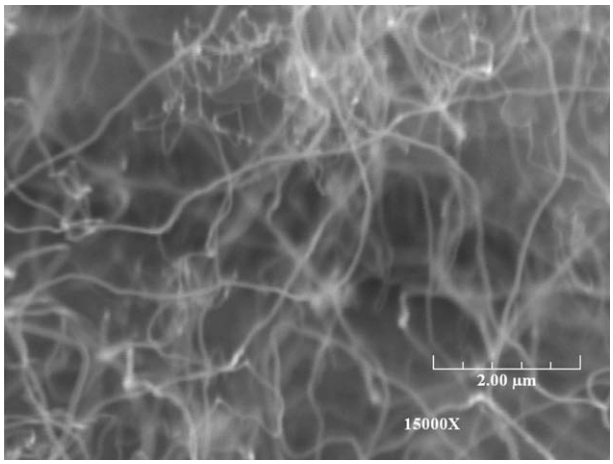

Fig. 3. Scanning electron micrograph (SEM) image of multi walled carbon nanotube (MWCNT) coated on a silicon wafer that was used for the flow boiling experiments.

4. Data analysis

MATLAB® software was used for analyzing the acquired transient temperature data. The wall heat flux data is obtained by calculating the spatial gradient of the temperature in the vertical direction at different radial locations within the copper cylinder:

$$q = k\frac{\Delta T_i}{\Delta x_i} = k\frac{T_2 - T_1}{\Delta x} \quad (1)$$

5. Experimental uncertainty

The thermocouples that are inserted into the copper block are calibrated using a NIST calibrated mercury thermometer by immersing them in a constant temperature bath (that is stirred to maintain uniform temperature). The thermocouples are calibrated by maintaining the constant temperature bath at steady state at different temperatures. The experimental uncertainty for estimating the heat flux in the vertical direction within the copper cylinder was estimated using the Kline and McClintock (1953) method:

$$\frac{\omega_q}{q} = \left[\left(\frac{\omega_k}{k}\right)^2 + \left(\frac{\omega_{T1}}{T_2 - T_1}\right)^2 + \left(\frac{\omega_{T2}}{T_2 - T_1}\right)^2 + \left(\frac{\omega_{\Delta x}}{\Delta x}\right)^2\right]^{\frac{1}{2}} \quad (2)$$

The uncertainty in thermal conductivity is estimated to be 1%. The uncertainty machining accuracy is estimated to be within 100 μm, resulting in position uncertainty of 2%. The calibration of the thermocouples is performed with a temperature stability of ±0.01 °C, which provides a measurement uncertainty of ±0.09–0.37 °C (at 95% confidence level). Hence, the experimental uncertainty for the wall heat flux was estimated to range from ±16% at boiling inception to ±4% at the maximum heat flux point.

6. Experimental procedure

The DI water was boiled in the constant temperature bath for 30 min prior to each experiment for degassing. After the degassing step a centrifugal pump was used to pump water into the test section. At this point the calorimeter apparatus was started. The flow rate of the pumps was adjusted using a rheostat. The flow meter was used to constantly monitor and adjust any variations in the pump flow rate. The temperature in the calorimeter was monitored using the digital data acquisition system. After steady state conditions were reached the temperature data from the thermocouples were recorded for 1 min. The power supply to the calorimeter was incremented by 5 V after each steady state condition.

7. Experimental results and discussion

Flow boiling experiments were performed using de-ionized (DI) water for liquid inlet temperatures of 40 °C and 60 °C (subcooling of 60 °C and 40 °C, respectively) and at two different flow rates of 0.13 and 0.17 l/s (mass velocities of 18 and 25 kg/m^2 s). The liquid flow only Reynolds numbers (Re_{le}) corresponding to these two flow rates are 2300 and 4300, respectively. The flow boiling heat flux data measured by the calorimeter was compared for the bare silicon substrate and the MWCNT coated substrate. The heat flux data for different experimental conditions were compared in this study.

7.1. Heat flux data

The heat flux in the copper block in the vertical direction was calculated for each steady condition at different wall temperatures using Eq. (1). The heat flux is plotted as a function of the copper block top surface temperature in Figs. 4–6. Since the top surface temperature of the silicon substrate (bare and coated with MWCNT) could not be measured in this study, the plots are shown with respect to the copper block top surface temperature. The data for flow boiling of silicon in Figs. 4–6 correspond to a mass velocity (G = 18 kg/m^2 s and liquid subcooling of 40 °C). Table 1 lists the heat flux enhancements between bare silicon wafer and the MWCNT coated heater at different flow rates and subcooling. The percentage enhancement was calculated by interpolating the heat flux data from MWCNT experiments at a particular heater temperature for which the experimental data from bare silicon

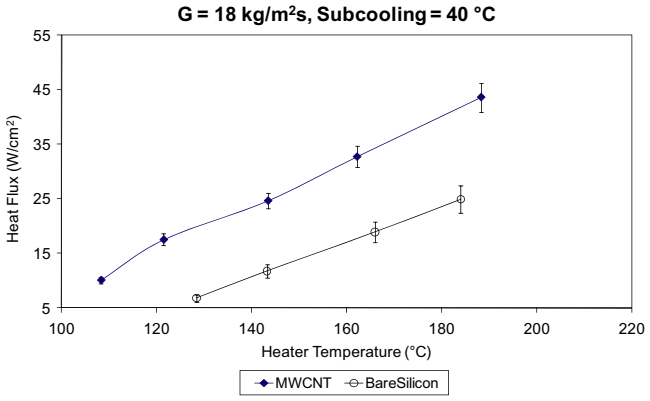

Fig. 4. Flow boiling heat flux is plotted as a function of the calorimeter (copper block) top surface temperature for bare silicon substrate and silicon substrate coated with MWCNT. The mass velocity of liquid at inlet is 18 kg/m^2 s and the water inlet temperature is 60 °C (liquid subcooling of 40 °C).

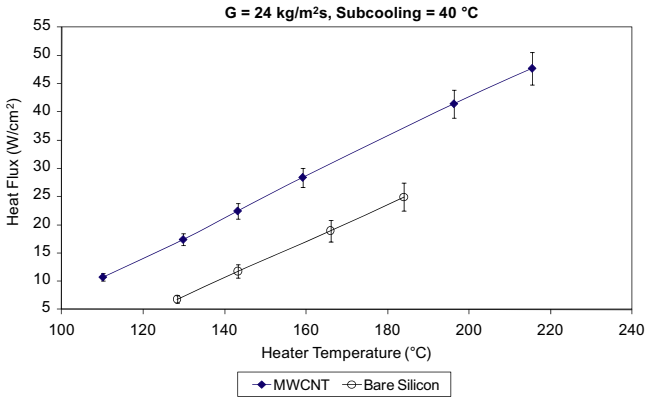

Fig. 5. Flow boiling heat flux is plotted as a function of the calorimeter (copper block) top surface temperature for bare silicon substrate and silicon substrate coated with MWCNT. The mass velocity of liquid at inlet is 24 kg/m^2 s and the water inlet temperature is 60 °C (liquid subcooling of 40 °C).

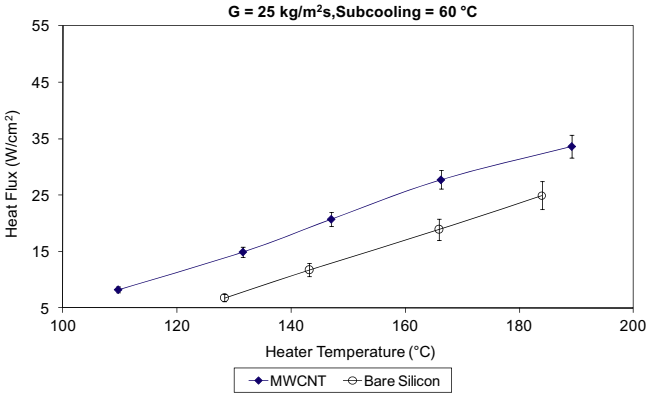

Fig. 6. Flow boiling heat flux is plotted as a function of the calorimeter (copper block) top surface temperature for bare silicon substrate and silicon substrate coated with MWCNT. The mass velocity of liquid at inlet is 25 kg/m^2 s and the water inlet temperature is 40 °C (liquid subcooling of 60 °C).

Table 1
Heat transfer enhancement with MWCNT (over bare silicon).

Heater temperature (°C)	G = 18 kg/m^2 s (ΔT)sub = 40 °C (%)	G = 24 kg/m^2 s (ΔT)sub = 40 °C (%)	G = 25 kg/m^2 s (ΔT)sub = 60 °C (%)
128	180	152	112
143	113	91	64
166	82	61	41
184	68	48	31

experiments were available (i.e., at 128 °C, 143 °C, 166 °C, and 184 °C). The heat flux value was interpolated between two nearest experimental data points for a given heater temperature. Table 1 shows that the MWCNT coating is more effective in enhancing heat flux at lower flow rates and lower values of liquid subcooling when compared to heat flux data obtained for bare silicon surface (at G = 18 kg/m^2 s and liquid subcooling of 40 °C).

Fig. 4 compares the heat flux obtained for MWCNT coated surface at G = 17.9 kg/m^2 s and liquid subcooling of 40 °C. It is observed that the MWCNT coating enhances the flow boiling heat flux in the fully developed nucleate boiling regime (bubbly flow regime) by 70–80% as the heater temperature is increased. Fig. 5 compares the heat flux obtained for MWCNT coated surface at G = 24.7 kg/m^2 s and liquid subcooling of 40 °C. It is observed that the MWCNT coating enhances the flow boiling heat flux in the fully developed nucleate boiling regime (bubbly flow regime) by 50–60% as the heater temperature is increased. This shows that there is a marginal decrease in the heat flux enhancement between coated and uncoated heaters as the flow rate is increased. Fig. 6 compares the heat flux obtained for MWCNT coated surface at G = 24.7 kg/m^2 s and liquid subcooling of 60 °C. It is observed that the MWCNT coating enhances the flow boiling heat flux in the fully developed nucleate boiling regime (bubbly flow regime) by 30–40% as the heater temperature is increased. This shows that MWCNT is less effective in enhancing flow boiling heat flux as the flow rate as well as the liquid subcooling is increased, for the range of experimental parameters utilized in this study. This behavior is consistent with saturated and subcooled pool boiling experiments reported in the literature. Ahn et al. (2006a,b) showed that the MWCNT coatings were more effective in enhancing pool boiling heat flux on horizontal heaters during saturated boiling than during subcooled boiling.

7.2. Boiling incipience

It is apparent from Figs. 4–6 that MWCNT is more effective at initiating boiling incipience at a lower value of the heater temperature than bare silicon substrates. This is to be expected since the silicon wafer surface is atomically smooth (a single crystal plane is exposed in these wafers). In contrast MWCNT coating provides a wide distribution of nano-scale nucleating cavities (due to distance between the individual nanotubes) along with micron-scale surface roughness (due to variation in height of the nanotubes). Therefore, it is expected that the nucleation site density will be orders of magnitude less on the bare silicon wafer than the MWCNT substrate. In this study the atomically smooth silicon wafer does not have any cavities for nucleation to occur. Consequently, higher wall superheats are required for nucleation incipience on the silicon wafers. Nucleation was observed to initiate on the periphery of the bare silicon wafer. Following the nucleation at the periphery – additional nucleation was observed on the whole wafer surface at higher wall superheats. Fig. 7 shows the bubble distribution at boiling incipience. The figure shows sparse nucleation on the wafer surface with higher density of nucleation at the edges of the wafer.

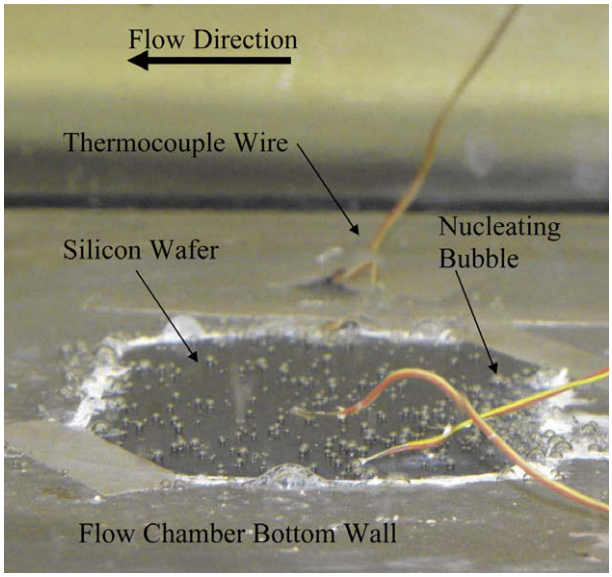

Fig. 7. Image of bare silicon wafer at boiling incipience.

The MWCNT was highly effective in enhancing the flow boiling heat flux at boiling incipience than in the fully developed nucleate boiling (bubbly flow) regime. At G = 17.9 kg/m^2 s and liquid subcooling of 40 °C the MWCNT coating enhanced the flow boiling heat flux at boiling incipience by 180%. At G = 24 kg/m^2 s and liquid subcooling of 40 °C the MWCNT coating enhanced the flow boiling heat flux at boiling incipience by 150%. And finally, at G = 25 kg/m^2 s and liquid subcooling of 60 °C the MWCNT coating enhanced the flow boiling heat flux at boiling incipience by 112%.

This trend in boiling incipience for flow boiling is contrary to the trend observed in pool boiling. Experiments by Ahn et al. (2006a,b) showed that the MWCNT more effective in enhancing pool boiling heat flux at higher wall superheats and especially at critical heat flux (CHF). This can be explained by using the models for flow boiling (Rosenhow, 1953) and nucleate boiling (Rosenhow, 1952). Rosenhow (1953) proposed that the total heat flux in flow boiling is composed of two components: that due to single phase liquid convection (q_{spl}) and that due to nucleate boiling (q_{nb}). Rosenhow assumed that at fully developed nucleate boiling (or in bubbly flow regime) the two components contribute to the total heat flux fairly independent of each other. It was proposed that the single phase component can be calculated using a conventional estimate for single phase internal flow heat transfer coefficient, e.g., Dittus and Boelter (1930) correlation (Incropera and Dewitt, 1996). If the liquid flow only Reynolds number (Re_{le}) is in the laminar flow regime, the heat transfer coefficient can be estimated by assuming the Nusselt number to be 4.36 (constant heat flux boundary condition) or 3.66 (constant surface temperature boundary condition). The additional nucleate boiling contribution to the total heat flux can be calculated using the Rosenhow (1962) correlation. In pool boiling there is no convective contribution. Hence, the heat flux increases with wall superheat. Rosenhow proposed the incorporation of a surface factor (C_{sf}) to account for surface wettability issues. Based on heat flux data from pool boiling experiments, Sathamurthy and Banerjee (2007) estimated the value of C_{sf} for MWCNT coated substrates to be 0.0034 and for bare silicon substrates to be 0.003. Hence – MWCNT is found to enhance pool boiling heat flux at higher values of wall superheat.

In contrast during flow boiling the boiling incipience is characterized by more complex transport processes. At boiling incipience the two components of heat flux (convective single phase and nucleate boiling) are of comparable magnitude and are highly

interdependent. Bubble nucleation can alter the effective surface roughness and wall shear stress profile and therefore augment the single phase convective component. In turn the single phase component of heat flux can also affect the temperature distribution near the wall (can cause the temperature gradients to be steeper at the wall). This can suppress nucleation for very smooth surfaces. MWCNT surfaces consist of protruding nano-structures that act like "nano-fins". This increases the effective surface area near the wall causing more rapid growth of the thermal boundary layer in the liquid phase leading to more enhanced density and frequency of bubble nucleation. Hence, MWCNT are found to be more effective in enhancing flow boiling heat flux at boiling incipience.

MWCNT are found to be less effective in enhancing heat flux at higher flow rates and higher liquid subcooling for similar reasons as enumerated above. At higher mass velocities the shear stress near the wall increases. This leads to formation of thinner boundary layers. Thus, the nucleation density of bubbles is reduced along with the decrease in bubble growth rates and departure frequencies. The single phase convective component is therefore more effective in transporting heat away from the wall, especially in the presence of the "nano-fins" (MWCNT). At higher subcooling the temperature differential is higher between the heater and liquid in contact – leading to higher heat flux for the single phase convective component. There is additional convective heat transfer between the liquid phase and the liquid vapor interface at higher subcooling (this component of heat flux does not exist for saturated boiling). This single phase component is enhanced further due to the presence of MWCNT coating. Hence, for the same wall temperature – at higher subcooling and at higher flow rates the single phase convective component of the total heat flux is able to transport a higher proportion of the total heat flux – which is at the expense of the nucleate boiling component.

It is unlikely that the MWCNT structures at the wall are distorted (or bent) significantly at higher mass flow rates since the mechanical rigidity of these nano-structures are higher than that of steel. Hence, the marginal enhancement of the shear stress at the wall (associated with higher mass velocities) is unlikely to cause any significant enhancement in strain on these structures. Also, these nano-structures reside within the "inner layer" of the turbulent boundary layer where the liquid momentum flux is negligible (compared to the free stream flow). Hence, increase in liquid momentum (associated with higher mass velocities) is unlikely to cause any significant distortions in these nano-structures.

8. Conclusion

Flow boiling heat flux was measured on bare atomically smooth silicon substrates and substrates coated with MWCNT that was synthesized in situ on the substrates using chemical vapor deposition (CVD) techniques. Experiments were performed for two different flow rates and two different values of liquid subcooling. The results can be summarized as follows:

1. It was observed that in the fully developed nucleate boiling regime (bubbly flow) the flow boiling heat flux was enhanced by 30–80%.
2. The enhancement levels were higher at lower flow rates and lower values of subcoolings.
3. The MWCNT was more effective in enhancing the flow boiling heat flux at boiling incipience. Heat flux was enhanced by 112–180% at boiling incipience when compared with bare silicon wafer.
4. The onset of boiling incipience was found to occur at lower values of heater temperature for the MWCNT compared to that for bare silicon wafers.

This behavior can be explained by using Rosenhow (1953) model by partitioning the total flow boiling heat flux into single phase forced convective heat flux in the liquid and nucleate boiling heat flux into the vapor phase. At boiling incipience the single phase and nucleate boiling component mutually augment each other. At higher mass velocities and liquid subcooling the MWCNT "nano-fins" contribute a higher proportion of the total heat flux to the single phase forced convective heat flux and therefore less effective in enhancing the total heat flux.

Acknowledgments

This work was supported by the United States Office of Naval Research. The authors thank Mr. I. Ramirez for his help with the assembly of the experimental apparatus. The authors thank Mr. M. Sunder for help with setting up the instrumentation for the experiments and the schematic drawings used in this paper. The authors also thank Mr. R. Gargate for his help with characterizing the MWCNT samples and for obtaining the SEM images of the MWCNT samples. The help of Mr. Pratanu Roy in obtaining Fig. 7 is also acknowledged. FE-SEM acquisition at the Microscopy and Imaging Center (MIC) at Texas A&M University was supported by the National Science Foundation under Grant No. DBI-0116835.

References

Ahn, H.S., Vijaykumar S., Banerjee, D., Lau, S., 2006a. Pool boiling experiments on multi walled carbon nanotubes and using surface-micromachined temperature sensors. In: Proceedings of the AIAA/ASME Joint Thermophysics Conference, San Francisco, CA, June 3–8.

Ahn, H.S., Sinha, N., Zhang, M., Feng, S., Banerjee, D., Baughman, R., 2006b. Pool boiling experiments on multi walled carbon nanotube (MWCNT) forests. ASME Journal of Heat Transfer 128 (12), 1335–1342.

Bakhru, N., Lienhard, J.H., 1972. Boiling from small cylinders. International Journal of Heat and Mass Transfer 15, 2011–2025.

Banerjee, D., Dhir, V.K., 2001. Study of sub cooled film boiling on a horizontal disc. Part I: analysis. Journal of Heat Transfer 123, 271–284.

Carey, V.P., 2007. Liquid Vapor Phase Change Phenomena, second ed. Taylor and Francis.

Dhir, V.K., 1993. Heat transfer. McGraw-Hill Encyclopedia of Science and Technology, 169–171.

Dhir, V.K., 1998. Boiling heat transfer. Annual Review of Fluid Mechanics 30, 365–401.

Dhir, V.K., Lienhard, J.H., 1973. Hydrodynamic prediction of peak pool boiling heat fluxes from finite bodies. Journal of Heat Transfer 95, 152–158.

Dittus, F.W., Boelter, L.M.K., 1930. Publications on Engineering, vol. 2. University of California Berkeley Press. p. 443.

Incropera, F.P., Dewitt, D.P., 1996. Fundamentals of Heat and Mass Transfer, fourth ed. Wiley Pub. pp. 445.

Kim, P., Shi, L., Majumdar, M., McEuen, P.L., 2001. Thermal transport measurements of individual multiwalled nanotubes. Physical Review Letters 87, 1–4.

Kline, S.J., McClintock, F.A., 1953. Describing uncertainties in single sample experiments. Mechanical Engineering 75 (1), 38.

Rosenhow, W.M., 1952. A method of correlating heat transfer data for surface boiling of liquids. Transactions of the ASME 84, 1969.

Rosenhow, W.M., 1953. Heat transfer with evaporation. In: Heat Transfer Symposium, University of Michigan Ann. Arbor. pp. 101–150.

Sathamurthy, V., Banerjee, D., 2007. Subcooled pool boiling studies on nanotextured surfaces. In: Proceedings of the InterPACK 2007, July 8–12, Vancouver, British Columbia (Paper No. IPACK2007-1936).

Sririaman, S.R., Banerjee, D., 2007. Pool boiling studies on nano-structured surfaces. In: Proceedings of ASME-IMECE, November 11–15, Seattle, WA (Paper No. IMECE2007-42581).

Thome, J.R., 1990. Enhanced Boiling Heat Transfer. Hemisphere Publishing, New York.

Webb, R.L., 1994. Principles of Enhanced Heat Transfer. John Wiley and Sons, New York, NY (Chapter 13).

Zhang, L., Shoji, M., 2003. Nucleation site interaction in pool boiling on the artificial surface. International Journal of Heat and Mass Transfer 46, 513–522.

Zhang, M., Atkinson, K.R., Baughman, R.H., 2004. Multi-functional carbon nanotube yarns by downsizing and ancient technology. Science 306, 1358–1361.